

The tower leg's anchoring capacity embedded in a concrete column surrounded by steel pipe subjected to uplift load

S.Saito

Tokyo Electric Power Services co., Ltd, Tokyo, Japan

S.Komiyama & S.Tanabe

Tokyo Electric Power Co., Inc., Tokyo, Japan

M.Matsushima

Kagawa University, Kagawa, Japan

ABSTRACT: A transmission tower leg is usually embedded in concrete column foundation, as shown in Figure 1. The leg is attached four and more ribs to anchor the concrete body. The anchoring capacity is determined chiefly by splitting cracks radiating from the leg. This report shows, if the concrete column is surrounded by steel pipe, when the radial splitting cracks occur in the concrete body, the surrounding steel resists to the failure of the anchor and anchoring capacity is largely increased. From the result of experimental study and simulation we have found out the followings. A pressure plate, which is welded to the top of the steel pile surrounding a concrete column, is necessary to prevent the concrete body from slipping at the boundary between the concrete body and the steel pile. Concrete body pressures the pressure plate, when the uplift load is transferred from the tower leg to concrete. Then, radial splitting cracks are developed by the circumferential tensile stress by the uplift load. Those radial splitting cracks propagate toward the surface of steel pile with increasing of uplift load and the number of splitting crack and crack width are increased at the upside face of concrete body. Concrete body is expanded in circumferential direction by splitting crack and the head of steel pile is radiated due to the internal pressure. The steel pile and the pressure plate are yielded in circumferential direction, and then the leg is pulled out suddenly. The quasi-3 dimensional analysis in this paper, which is based on fracture mechanics and basically the same as the one we reported in Framcos3 (cf. reference), is verified to be useful tool by comparing results of experiments and computations.

1 INTRODUCTION

Many reports on the method to anchor into a concrete block foundation have been published in recent years. We have developed the anchorage method of caisson type foundation for transmission towers used pipes with rib embedded into the foundation body as shown in Fig 1. According to previous studies, a splitting failure caused by circumferential tensile stress can be observed when an uplift load is subjected. We developed a new anchorage method of pile foundation using a steel pipe with pressure plate as shown in Fig.2. The pressure plate is placed at the top of the steel pile and the concrete is filled up between a leg and a steel pipe not so as to get out from the pile body. The uplift load caused by wind force acting tower is transmitted at legs of tower. Therefore, the leg of tower, which is a steel pipe with ribs, is embedded in the foundation body as an anchorage. This paper describes the simulation of behavior of anchor embedded in concrete body subjected to uplift load using the proposed finite element analysis.

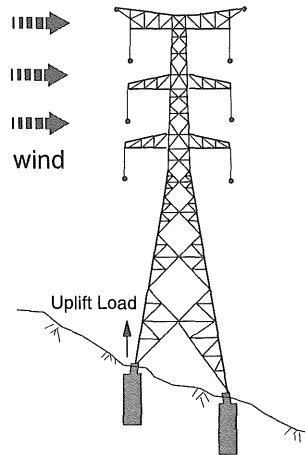


Figure 1. Transmission Tower

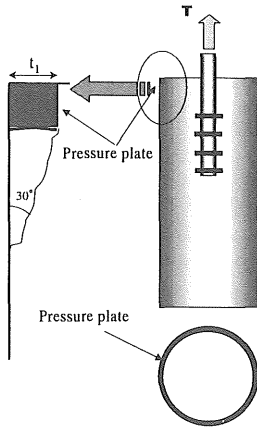


Figure 2. New Developed Anchorages

2 EXPERIMENTS

2.1 Specimens

Outline of specimen is shown in Fig 3. The steel pipe modeled as an anchorage of tower legs is diameter 120mm with thickness 18mm and the rib is diameter 140mm with thickness 3.2mm. Steel pile modeled as foundation pile is diameter 609.6mm with thickness 3.2mm. The 25mm wide plate with thickness 19mm modeled as a pressure plate is placed at the top of the steel pile. The target compressive strength of concrete is $f_c' = 24 \text{ N/mm}^2$. The parameter of specimen is pressure plate size as shown in Tab 1. Pull out test of two specimens is carried out due to the comparison with the result of numerical analysis mentioned below chapter.

2.2 The result of experiments

The relationship between load and displacement of each specimen shows Fig 4. The ultimate load of specimen K-1b and K-3 indicates 754kN and 1070 kN respectively and varied with the size of pressure plate placed at the top of steel pile. Fig 5 and Fig 6 indicate the state of cracking pattern of each specimen at the ultimate load. Specimen K-1b shows that concrete filled up in steel pile is overstuffed and radial cracking occurs at the concrete surface of pile head. The steel pile gets longer in the circumferential direction by expanding of a concrete body. Cross section of specimen due to observing the state of cracking is cut off. Fig 7. and 8. show the cracking state of cross section respectively. Since the shear cracking pattern occurs from the top of each rib at 45° direction, it seems that the shear force may transmit from the rib attached at the leg to steel pile through concrete body. According to strain gages of the steel pile, the strain at the head of steel pile in circumferential direction is increasing with uplift

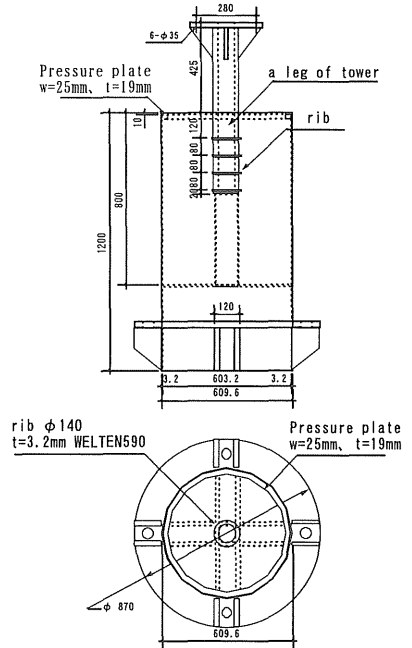


Figure 3. Outline of Specimen

Table 1. Parameters

Specimen	Pressure Plate	Pressure Plate
	Width	Thickness
	mm	mm
K-1b	12	4.5
K-3	25	19

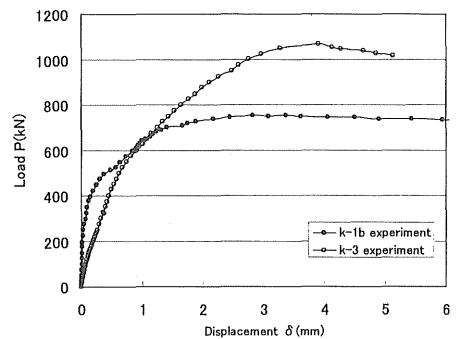


Figure 4. Load-Displacement Relationship

load and the head of steel pile is deformed as bell shape by the increasing of stress in circumferential direction. The idea of failure mechanism is shown in Fig 9. The head of steel pile and the pressure plate are yielded by the stress in circumferential direction generated by the horizontal component force of internal pressure transmitted from ribs attached to the leg. The leg slips out of concrete body with the

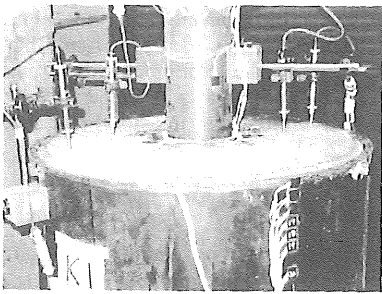


Figure 5. States of Cracking (Specimen K-1b)

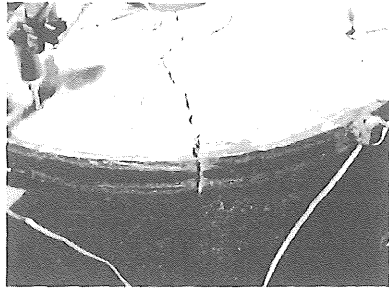


Figure 6. States of Cracking (Specimen K-3)

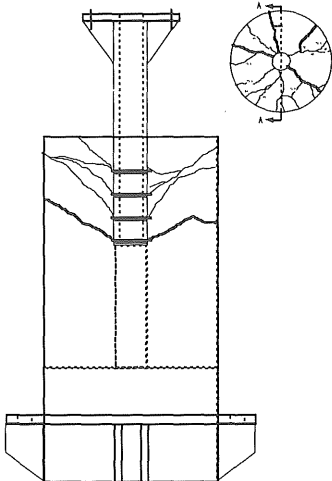
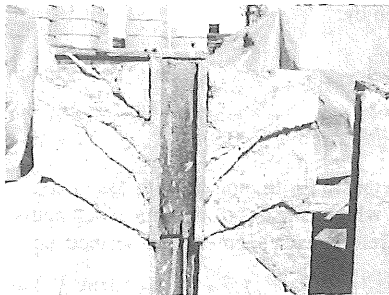


Figure 7. States of Inner Cracking (Specimen K-1b)

propagating of splitting crack. Therefore, it is judged that the ultimate capacity may be govern by the yielding of steel pile head in circumferential direction.

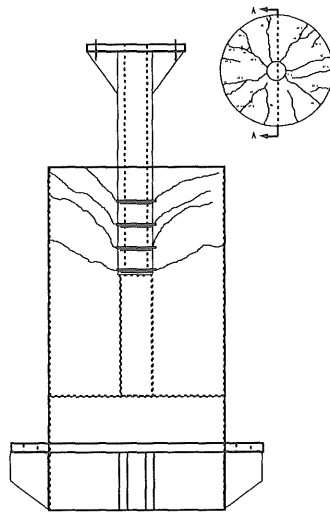
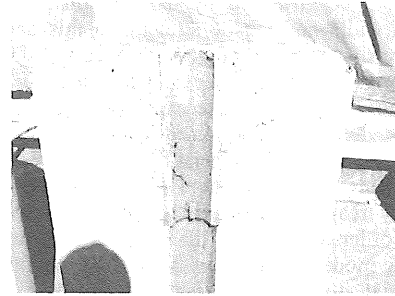


Figure 8. States of Inner Cracking (Specimen K-3)

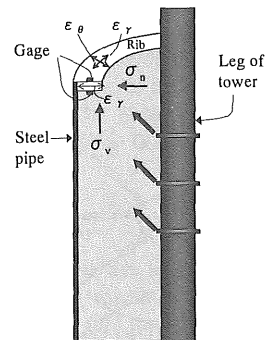


Figure 9. Idea of Failure Mechanism

3 SIMULATION

3.1 Numerical method

Uplift load transmits from ribs attached with the leg to the concrete body. The circumferential force propagates splitting cracks. The splitting cracks assume to be governed by the relationship between crack width and tensile strength in this paper. The failure of concrete body is not occurred due to the confinement of steel pile and the yielding of steel pile governs the ultimate capacity. Therefore, Von-Mises yield criterion is used in the yielding of steel pile. The three dimensional behavior of the concrete body subjected uplift load assumes to be approximately treated with an axially symmetric model.

In order to carry out the analysis of axially symmetric model, a mean stress-strain model in circumferential direction is used an out-plane cracking model with considering the effect of splitting crack. A smeared crack model is used as an in-plane cracking model with considering the shear crack width.

It is well known that concrete does not immediately release stress after cracking but gradually releases the stress corresponding to crack width as shown in Fig 10. The behavior of concrete after cracking is described by assuming that the relationship between crack width and tensile stress may be

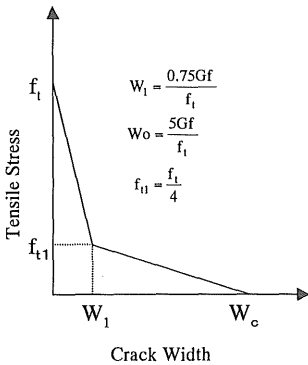


Fig 10. Tension Softening Characteristics

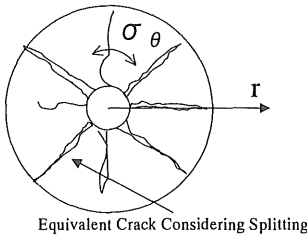


Fig 11. Splitting Cracks Observed in Experiment

modified as the bi-linear model with tension softening curve shown in Fig 10. Several splitting cracks were observed in the experiments. The number of cracks in the simulation is assumed to be eight as eight cracks were seen in most experiments as shown in Fig 11.

3.2 Constitutive equation of splitting crack

The mean stress-strain relationship in circumferential direction can be obtained by assuming that the stress of a concrete cylinder in circumferential direction is uniform. Displacement in the circumferential direction δ_θ can be described by the summation of the displacement generated by eight splitting cracks' widths and the elastic displacement of concrete without cracking generated by the circumferential stress σ_θ at radius r as shown in Fig. 11. Therefore, δ_θ is given by Eq.(1).

$$\delta_\theta = nw + \frac{\sigma_\theta}{E} 2\pi r \quad (1)$$

where, n : number of cracks, E : Young's modulus of concrete, w : crack width. Therefore, the mean strain is given by:

$$\bar{\epsilon}_\theta = \frac{\delta_\theta}{2\pi r} = \frac{nw + \frac{\sigma_\theta}{E} 2\pi r}{2\pi r} \quad (2)$$

The tension softening curve is assumed as the model which consists of two linear segments.

Therefore, each segment is described as:

$$\sigma_\theta = aw + b \quad (3)$$

The mean stress-strain relationship in circumferential direction is obtained by using Eq.(2) and Eq.(3). The mean stress σ_θ can be obtained from Eq.(4) as:

$$\bar{\sigma}_\theta = \frac{1}{\frac{n}{2\pi ar} + \frac{1}{E}} \left(\bar{\epsilon}_\theta + \frac{nb}{2\pi ar} \right) \quad (4)$$

The mean stress-strain relationship in circumferential direction corresponding to Fig 10 is obtained the tri-linear curve as shown in Fig 12 using above Eq.(4).

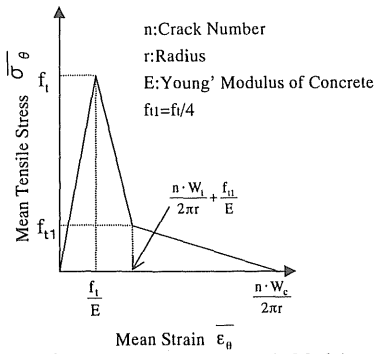


Figure 12. Mean Stress- Strain Model

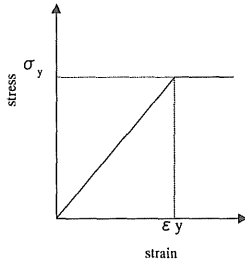


Figure 13. Model of Steel Pile

3.3 In-plane crack Model

In order to apply the tension softening model to in-plane crack model, the splitting crack is modeled by changing the $w - \sigma$ relationship to $\epsilon - \sigma$ relationship in each element width as shown in Fig. 12.

3.4 Model of steel pipe

The model of steel pile is used Von-Mises rule as yielding criteria and the stress-strain relationship is used bi-linear model as shown in Fig 13.

3.5 Model of Specimen

The finite element meshes of pipe, ribs, concrete cylinder, pile and pressure plate in the analysis are modeled as shown in Fig 14(a) and (b). The three-dimensional behavior of the concrete cylinder subjected to uplift load can be approximately treated with an axially symmetric model using the mean stress-strain relationship involving splitting cracks in circumferential direction. Shear reinforcements in the concrete cylinder is neglected because few reinforcements are used. An analytical model can be derived by using isoparametric elements with four nodes for pipe, ribs, concrete cylinder, pile and pressure plate. The interface between pipe or rib and concrete cylinder can be modeled by joint elements considering slip at the interface. The bottom of the

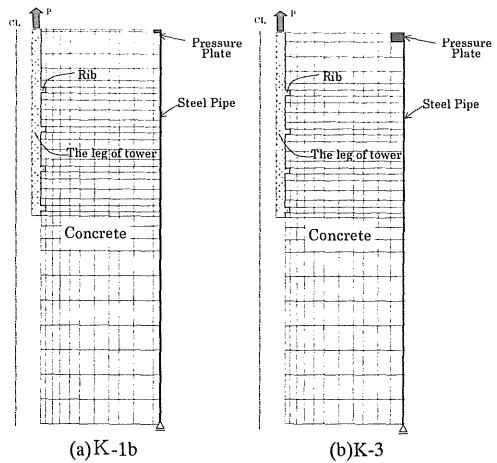


Figure 14. Finite Element Mesh

Table 2. Material Properties of Concrete

Compressive Strength f_c N/mm ²	Tensile Strength f_t N/mm ²	Young's Modulus E_c kN/mm ²	Fracture Energy G_F N/mm
33	2.8	28	0.1

Table 3. Material Properties of Steel Pile

Yield Strength F_y N/mm ²	Young Modulus E_c kN/mm ²	Poisson's Ratio ν
260	200	0.3

pile is restricted. The analysis is carried out to pull out the leg in vertical direction using controlling the displacement. In order to consider the elasto-plastic deformation of pipe, ribs, pile and pressure plate elasto-plastic model based on the Von-Mises yield criterion is used. The concrete is assumed to be elastic until cracking occurs. The Drucker-Prager yield criterion is used in concrete subjected to compressive stress. Cracking is described by a smeared cracking model in this paper. Normal stiffness to splitting crack is assumed to be governed by the mean stress-strain relationship as shown in Fig. 12. Shear stiffness is assumed to decrease to one tenth of the initial stiffness after shear crack occurs. Table 2.3 shows the parameters of material properties of concrete and pile.

3.6 Results of Analysis

Fig.15 and 16 show the load-displacement relationship of numerical results and experimental results. It can be judged that the splitting crack of concrete body reaches the face of steel pile because the load-displacement relationship declines at 640kN in numerical analysis of specimen K-1(b). After that, the load increases in numerical analysis and the ul-

timate load indicates 836kN. The ultimate load in experiment indicates 754kN. The result of load-displacement coincides with the experiment although the ultimate load has a difference of 11%.

The load-displacement of specimen K3 in numerical analysis also declines at 670kN because splitting crack of concrete body reaches the face of steel pile. After then, the load increases in numerical analysis and the load-displacement relationship of experiment and computation nearly coincides until the ultimate load in numerical analysis. The ultimate load in experiment indicates 1070kN and the results of load-displacement relationship coincide with numerical analysis although the ultimate load has a difference of 8%.

Fig. 17(a),(b),(c) and (d) show the computational results of deformation, cracking in circumferential direction, propagation of plastic zone and principal stress in cross section of specimen K-1b. Step 29 indicates the ultimate load. Step 40 indicates after the ultimate load. The deformation of concrete body around the leg governs the displacement in vertical direction. However, it is found out that the upper part of concrete body is deformed at Step 29 and the steel pile is deformed as the bell shape. The reason

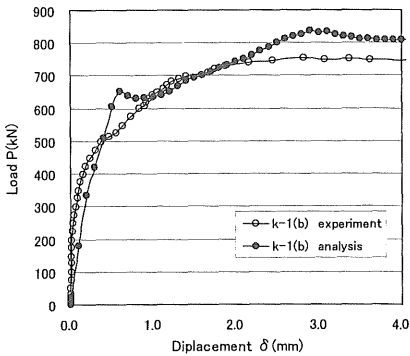


Figure 15. Load-Displacement (Specimen K-1b)

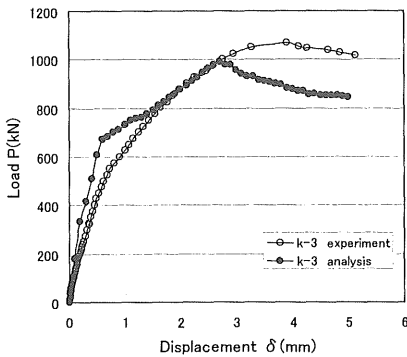
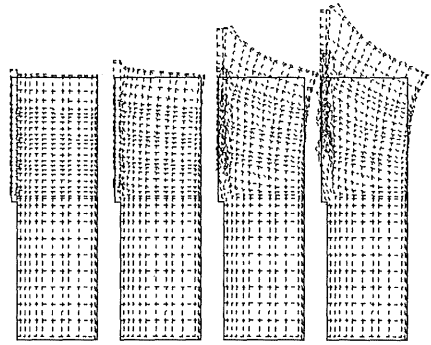
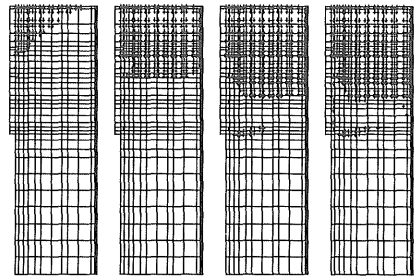


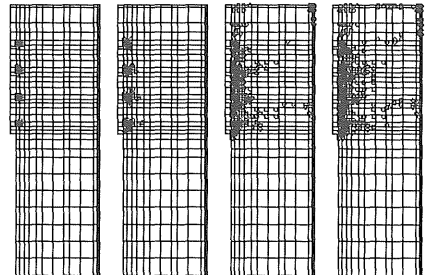
Figure 16. Load-Displacement (Specimen K-3)



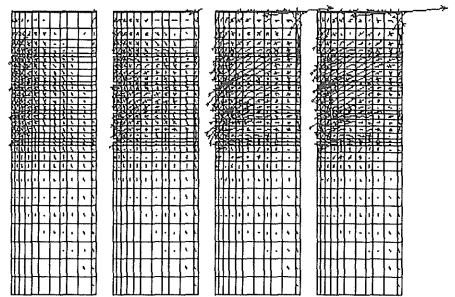
<STEP= 5> <STEP=10> <STEP=29> <STEP=40>
Figure 17(a). Deformation (Specimen k-1b)



<STEP= 5> <STEP=10> <STEP=29> <STEP=40>
Figure 17(b). Cracking in Circumferential Direction (Specimen k-1b)



<STEP= 5> <STEP=10> <STEP=29> <STEP=40>
Figure 17(c). Propagation of Plastic Zone (Specimen k-1b)



<STEP=5> <STEP=10> <STEP=29> <STEP=40>
Figure 17(d). Principal Stress in Cross Section (Specimen k-1b)

that the steel pile is expanded in circumferential direction as bell shape is due to the effect of splitting crack in computation. The splitting crack propagates from the head of concrete body toward the bottom with the increasing of loading as shown in Fig 17(b). The splitting crack does not propagate to the bottom of leg and this is same as the propagation of splitting crack in experiment. Fig 17(c) indicates the plastic area (yielding). The concrete on ribs describes the compressive failure. The pressure plate attached at the steel pile and the concrete around rib become to be plastic at Step 29. From the principal stress chart as shown in Fig 17(d), the uplift load is transferred from each rib toward concrete body. This direction is nearly same as the shear crack direction in experiment.

Fig. 18(a),(b),(c) and (d) show the computational results of deformation, cracking in circumferential direction, propagation of plastic zone and principal stress in cross section of specimen K-3.

The behavior of specimen K-3 is nearly same as the specimen K-1b mentioned above. The expansive displacement deformed as the bell shape is smaller than specimen K-1b by confinement of pressure plate because the thickness of pressure plate is larger than specimen K-1b.

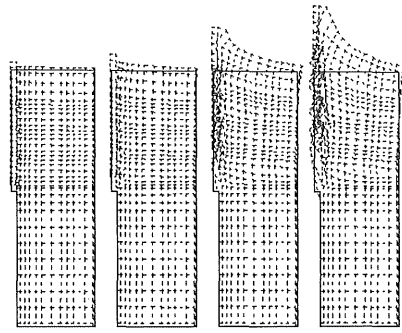
The concrete on the ribs indicate the compressive failure, but the ribs do not become to be yielding at ultimate load. Each rib is transferred load to the pressure plate through the concrete body. It is found that the principal stress in the bottom of concrete body is smaller than specimen K-1b.

Fig 19(a) and (b) shows the strain distribution of experiment and computation in circumferential direction. The strain of experiment and computation indicates zero until 50cm distance from the bottom of steel pile. This is the reason that the bottom rib is located at 50 cm distance from the bottom of the steel pile. The computed values are smaller than experiments although the tendency of both computed values are approximately simulated against experiments. The results of computation and experiment in specimen K-1b becomes not to be yielding. Although the result of computation in specimen K-3 becomes not to be yielding, the result of experiment becomes to be yielding at the ultimate load.

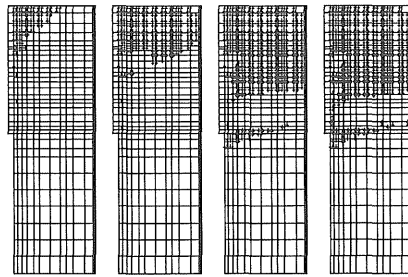
Fig. 20(a) and (b) show the strain distribution of legs in vertical direction. Although the numerical analysis has a scattering, the tendency of strain distribution coincides with experiment. However, the both numerical results are smaller than experiments.

4 CONCLUSIONS

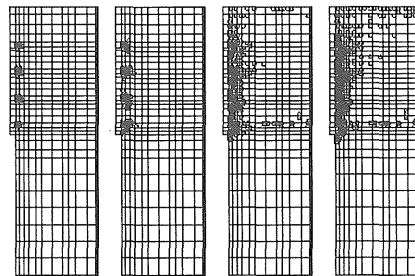
We develop the new anchorage method against the uplift load. Two specimens are carried out by the loading of uplift load. The behavior of results is



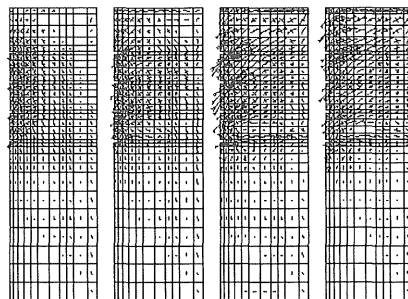
<STEP= 5> <STEP=10> <STEP=27> <STEP=40>
Figure 18(a). Deformation (Specimen k-3)



<STEP= 5> <STEP=10> <STEP=27> <STEP=40>
Figure 18(b). Cracking in Circumferential Direction (Specimen k-3)



<STEP= 5> <STEP=10> <STEP=27> <STEP=40>
Figure 18(c). Propagation of Plastic Zone (Specimen k-3)



STEP= 5 STEP= 10 STEP= 27 STEP= 40
Figure 18(d). Principal Stress in Cross Section (Specimen k-3)

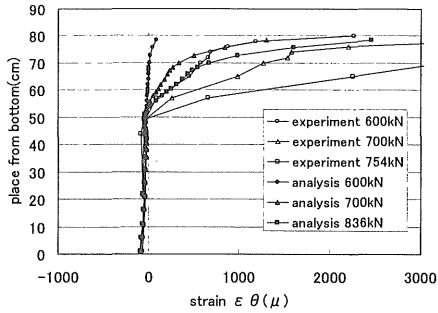


Figure 19(a). Strain Distribution in Circumferential Direction (Specimen k-1b)

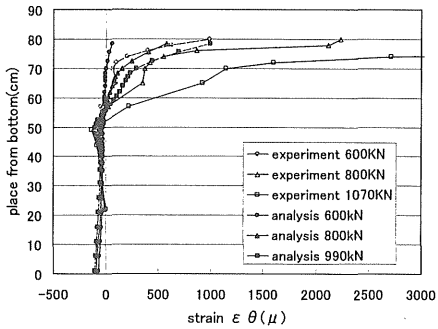


Figure 19(b). Strain Distribution in Circumferential Direction (Specimen k-3)

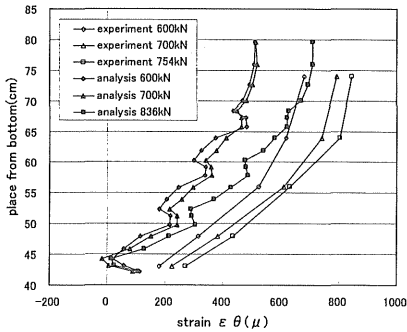


Figure 20(a). Strain Distribution in Vertical Direction (Specimen k-1b)

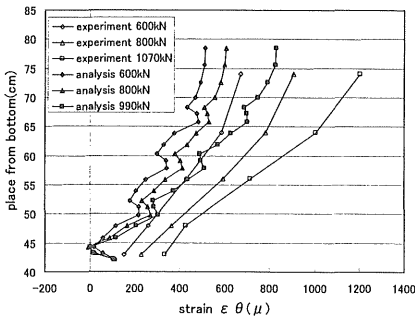


Figure 20(b). Strain Distribution in Vertical Direction (Specimen k-3)

simulated by using proposed finite element analysis based on fracture mechanics in this paper.

The findings in this paper are as follows:

- (1) The load-displacement relationship of specimens can be simulated using the proposed numerical model. The ultimate load of specimen K-1b has a difference of 11% and specimen K-3 is 8%.
- (2) The splitting crack in computation and experiment propagates from the head of concrete body toward the bottom with the increasing of loading. The splitting crack does not propagate to the bottom of leg and this is same as the propagation of splitting crack in experiment.
- (3) The tendency of strain distribution of the legs in vertical direction in computation coincides with experiment. However, the both numerical results are smaller than experiments.
- (4) The failure mode of experiments is governed by the yielding of steel pile and the ultimate bearing capacity in computation is also determined by the yielding of steel pile.

REFERENCES

- Yoshii, Y., Iijima, M., Saito, S. and Matsushima, M., 1998. Experimental study on bond of anchor pipe with ribs embedded in the caisson type foundation, JSCE, No.606/V-41:129-140
- Yoshii, Y., Iijima, M., Saito, S. and Matsushima, M., 1998. Numerical analysis on anchorage performance of pipe with ribs embedded in the caisson type foundation, JSCE, No.606/V-41:141-149
- Yoshii, Y., Tanabe, S., Ohura, A., An, X. and Mishima T., 1997: Finite Element Analysis of Pulling-out Behavior for RC Footing Supported by Four Piles, Proceeding FRAMCOS-3.
- Yoshii, Y., Iijima, M., Komiyama, S., Saito, S. and Matsushima M., 1997. Finite Element Analysis of Anchorage Performance of Embedded in the Caisson Type Foundation Subjected to Uplift Load, Proceeding FRAMCOS-3.
- Sonobe, Y., Tanabe, S., Yokozawa, K. and Mishima, T., 1994. Experimental Study on Size Effect in Pull-out Shear using Full Size footings, in Size Effect in Concrete Structures, (eds H. Mihashi, H. Okamura and Z.P. Bazant), E&F.N. Spon, London, 105-116.
- JCI International Workshop on Size Effect in Concrete Structures. 1993. Sendai, Japan. JCI
- JCI committee. 1993. Application of Fracture Mechanics to Concrete Structures. Japan. JCI
- Committee on Post-Peak Behavior of RC Structures. 1999. Seminar on Post-Peak Behavior of RC Structures Subjected to Seismic Loads. Japan. JCI